

**Keywords:** pavement management; international roughness index; artificial neural networks; gene-expression programming; pavement performance assessment; road roughness indices

**Razan SBIAH<sup>1</sup>, Rana IMAM<sup>2\*</sup>, Mohammad ALHIARY<sup>3</sup>, Bara'AL-MISTAREHI<sup>4</sup>**

## **DEVELOPING PREDICTION MODELS FOR SLOPE VARIANCE FROM THE INTERNATIONAL ROUGHNESS INDEX**

**Summary.** Road roughness is considered a primary indicator of pavement condition and serviceability, and the performance of paved roads is linked to road roughness. The focus of this study is to develop a relationship between two important roughness indicators, namely the international roughness index (IRI) and slope variance (SV), based on actual road roughness data to achieve a suitable correlation between these two indices using artificial neural networks (ANNA) and gene expression programming (GEP) techniques. Different study areas were selected to develop the prediction model. The first study area is the Desert Highway in Jordan, while the three remaining study areas are located in the US. A total of 533 data sets were used in this study to develop a model to predict the IRI from the SV. The GeneXproTools 5 software package was used to build the GEP model, while MATLAB 2019 was employed to develop the ANN model. The results showed that the GEP and ANN models outperformed all other previous models. The GEP-Based model showed a better performance and more precise results than the ANN model according to the coefficient of determination ( $R^2$ ).

### **1. INTRODUCTION**

The progress of nations and communities is mainly related to transportation systems, especially road networks. Roads comprise a primary connection between countries to enhance the motion of passengers and the transfer of goods. In developing countries like Jordan, much attention is paid to improving the roads sector, as the transportation system generally consists of highway roads, given the shortage in other transportation systems like railway systems.

Therefore, the roads network in Jordan is continuously growing, thus requiring construction, evaluation, and maintenance [1]. Due to the rise in the number of vehicles and road users in Jordan, expenditures on the highway networks take up 76% of the government's infrastructure budget, while the other 24% is spent on maintenance [1]. The performance of paved roads is linked to road roughness, which is considered a primary indicator of pavement condition and serviceability. Today, many highways and pavement agencies measure road roughness and calculate appropriate road roughness indices to evaluate pavement serviceability and performance.

Periodic maintenance should be implemented to keep the performance of roads at an acceptable level, provide high-quality and enhanced services, and extend the life of roads. The level of road roughness

---

<sup>1</sup> The University of Jordan, Department of Civil Engineering, School of Engineering; Amman 11942, Jordan; email: razan.sbaih95@gmail.com; orcid.org/0000-0001-6064-4535

<sup>2</sup> The University of Jordan, Department of Civil Engineering, School of Engineering; Amman 11942, Jordan; email: r.imam@ju.edu.jo; orcid.org/0000-0003-4576-6053

<sup>3</sup> The University of Jordan, Department of Civil Engineering, School of Engineering; Amman 11942, Jordan; email: hiary430@gmail.com; orcid.org/0000-0002-4057-2228

<sup>4</sup> Jordan University of Science and Technology (JUST); Irbid 22110, Jordan; email: bwmistarehi@just.edu.jo; orcid.org/000-0001-8440-0690

\*Corresponding author. Email: [r.imam@ju.edu.jo](mailto:r.imam@ju.edu.jo)

affects the user's perception of the ride quality, the motion and operation of the moving vehicle, and the comfort of the user.

The concept of pavement irregularities or roughness was introduced 40 years ago in the pavement performance field. These indices are classified into two major groups. The first group is the vehicle type indices, such as the international roughness index (IRI), which is obtained from the conversion of the profile data of a single wheel path, and the quarter-car index (QI). The second group is direct surface roughness indices, such as the SV, which is used in the AASHTO road test and the root-mean-square vertical acceleration (RMSVA). Each roughness index represents a convenient index for monitoring pavement roughness deterioration over time.

Many researchers and practitioners have found correlations between pavement performance and the longitudinal surface roughness profile [2]. Road roughness has a strong influence on the public's judgment of road serviceability [3].

## 2. LITERATURE REVIEW

The focus of this study is on developing a relationship between IRI and SV using actual road roughness data from Jordan and the US to achieve a suitable correlation between these two indices. The IRI field measurement process and devices are less expensive and easier to use than the SV measurement process. Moreover, the IRI data are more available for various pavement road sections due to the availability of IRI measuring devices. Therefore, the need to use the IRI data to predict the SV values appeared since SV is considered an important parameter for estimating the present serviceability index (PSI), which is a fundamental aspect in the field of road design and maintenance.

In the early 1900s, pavement profile data were obtained from the straightedge device [4]. After that, other profiling equipment was developed, such as the profilograph and response type road roughness measuring system (RTRRMS). Many developments were observed for profile measuring devices by the highway agencies. The rod and level, dipstick, and Australian Road Research Board (ARRB) laser profiler are modern accurate, lightweight devices for profiling and are being recently used by many agencies. Chang [4] used ProVAL version 2.73 to compute the IRI of an extremely smooth 50-m long pavement using the ready-made robot. Imam et al. [5] used GEP models for the first time to predict the pavement condition index (PCI) from the IRI, using data that was half compiled from the existing literature, while the other half was measured and collected in the field by the authors. The GEP model outperformed all the other available models in the literature, with a maximum  $R^2$  of 82% for the complete dataset. Carey et al. [6] discussed and compared road roughness measuring devices. They described the CHLOE profilometer as the most efficient device for estimating the slope variance for road sections in the field.

Yunusov et al. [7] compared eight different road profiling devices to assess road roughness, including total station, laser profiler, accelerometers, a smartphone GY 61 with an in-house designed and developed data acquisition system and analogy-to-digital converter, and the Roughometer III from the ARRB group. The results of this study showed that the laser profile was more efficient and accurate than the other devices. It is an excellent and superior tool to measure road roughness and detect IRI values. Islam et al. [8] used ProVAL software to calculate pavement road roughness. They obtained vehicle acceleration data from the smartphone application and calculated pavement roughness for 0.1 miles using ProVAL along a 2-mile test section. The maximum IRI value was 141.5 in/mile, while the minimum IRI value recorded was 42 in/mile.

Arhin et al. [9] developed a statistical regression model linking the IRI and PCI for different pavement types and highway classifications, using data collected over a two-year period to establish the IRI-PCI model. Overall, 895 data points were employed and distributed; the optimal IRI-PCI regression model formed is shown in Eq. 1.

$$PCI = A(IRI) + K + \varepsilon \quad (1)$$

where: A and K = constants;  $\varepsilon$  = associated error.

Azim et al. [10] employed GEP to develop a prediction model for the compressive arch action capacity of reinforced concrete (RC) frame structures under a column removal scenario. The model

contained six input parameters correlated with compressive arch action (CAA) capacity. The data were collected from different sources and were later used to validate the model. The GEP model demonstrated superior performance to linear and non-linear regression methods.

Murad et al. [11] employed GEP techniques to propose compressive strength models for green concrete. They developed four different GEP models by employing a large and reliable database obtained from the literature. The GEP models achieved high  $R^2$  values and low root mean square error (RMSE) and MAE values, which indicates the capability of the GEP to make reasonably accurate predictions. Adams and Bahia [12] used multiple linear regression (MLR) and backpropagation neural network (BPNN) techniques to estimate pavement roughness (IRI). This study was performed on data from Texas, New Mexico, and Arizona. The ANN model achieved a high correlation and had fewer mean square errors (MSEs) than the MLR model. The MSE for MLR was 0.108, and it was 0.023 for the ANN model. The correlation coefficient was 0.68 for MLR and 0.85 for ANN.

Vidya [13] established a prediction model for IRI depending on the pavement condition index (PCI) using ANN. The study was conducted on 43 sections of the Trichy-Tanjavur National Highway 67 in India, which covers a total of 56.49 km. The average longitudinal profiles along single paths were measured for the selected highway using a machine for evaluating roughness using low-cost instrumentation (MERLIN). Then the IRI was obtained to express road roughness. The IRI was calculated using Eq. 2.

$$IRI = 0.593 + 0.0471D \quad (2.4 < IRI < 15.9) \quad (2)$$

where D is measured using the MERLIN chart.

In addition to IRI, the PCI of each selected section was obtained using Eq. 3[5]

$$PCI = 100 - CDV \quad (3)$$

where: CDV = corrected deduct value (less than 100).

This model recorded an  $R^2$  value of 0.86 and an MSE value of 0.041. The results showed that the neural network is recommended to predict the IRI for construction work zones since it is hard to obtain IRI values from the field.

Hossain [14] developed an IRI prediction model using ANN techniques for four flexible pavement sections with various climate conditions. The climate conditions were a dry-no freeze region, a wet-no freeze region, and dry and wet freeze regions. The data points were divided into two categories: 50% of the data was employed in the training process, and the other half was used for the testing process. The final ANN model achieved a high correlation between the IRI measured from data and the IRI predicted from the ANN model; the value of RMSE was 0.01. This confirmed that ANN techniques are reasonable and accurate for predicting the IRI from climate and traffic data only.

Mazari and Rodriguez [15] developed a roughness prediction model to forecast the IRI using a hybrid technique that combines GEP and ANN. The first roughness prediction model was developed using data taken from the long-term pavement performance (LTPP) database using the GEP technique. For this model, 80 records were employed for training, and the remaining 15 independent data records were used for validation. The technique achieved a high correlation coefficient ( $R = 0.9912$ ). For the other data, the ANN model achieved high correlation coefficients for both the training and validation datasets (0.9649 and 0.9562, respectively). These results show the effectiveness of GEP and ANN in predicting the IRI. Bayrak et al. [16] generated a prediction model of IRI using BPNN for rigid pavements. Data from nine US states and 83 sections were considered in this study. The results confirmed the usefulness of ANNs for modeling complex relationships. The model achieved accurate predictions of IRI, with an  $R^2$  of 0.84 for training data and 0.81 for testing data.

Dujisin and Arroyo [17] found a relationship between SV and IRI. They defined longitudinal slope variance as a parameter that represents the roughness of pavement sections and correlated these variances to the unevenness of the longitudinal profile. These variances were measured with a special piece of equipment called a profilometer. Their research employed the following procedures to obtain the relationship between SV and the IRI:

- 1 - Calculate the IRI and SV for the pavement profile using the World Bank computer program.
- 2 - Use AASHTO's equation to calculate the SV.
- 3 - Obtain the relationship between the IRI and SV and randomly generate a simulation for the pavement profile.

This procedure was repeated until a database of IRI-SV pairs was obtained. In this work, a database of 458 pairs of IRI-SV values was considered. Finally, statistical regression was used to relate these two variables, resulting in Eq. 4. This relationship achieved an  $R^2$  of 0.977.

$$\log(1 + SV) = 0.835 \text{ IRI}^{0.5} - 0.448 \quad (4)$$

Hall and Muñoz [18] investigated a model to evaluate the PSI as a function of the IRI. The model comprised two steps. The first step was developing the relationship between the SV and PSI values, and the second step was developing the relationship between SV and the IRI for asphalt and concrete pavement profiles using AASHTO road test performance models.

A relationship between SV and the IRI was established by Dujisin and Arroyo [17]. More than 400 profiles were used; each was represented by 1000 elevation points spaced at 1-ft intervals. The slope of each point was calculated using the normal distribution. Then, SV was computed as the population variance for slopes (multiplied by 1 million) for each profile. By analyzing the IRI-SV pairs, the regression (Eq. 5) was calculated as  $R^2 = 0.988$ . The advantage of this model is that it has a zero intercept without sacrificing the goodness of fit of the rest of the data range.

$$SV = 2.2704 \text{ IRI}^2 \quad (5)$$

where: IRI is in m/km.

Shahnazari et al. [19] investigated a prediction model to estimate the PCI value using a non-linear optimization technique, incorporating ANN and generic programming (GP). The study was conducted in Iran on a 1,250-km highway, where 12,487 distressed data points were collected, including fatigue, transverse, and longitudinal cracks. Although the two models achieved a high precision with low error, the ANN model was more accurate than the GP-based model. The ANN model recorded an  $R^2$  value of 0.9986 and a mean absolute error (MAE) of 0.49. On the other hand, the  $R^2$  value and MAE of the GP model were 0.9898 and 1.79, respectively.

Thus, there is high interest in measuring and computing road roughness. Therefore, many researchers have related the various roughness indices using different techniques. This study will focus on the relationship between the IRI and the SV to develop a highly correlated model for obtaining one index from the other. The two programs chosen in this research to develop this relationship and connect the two indices together were the ANN and the GEP.

### 3. RESEARCH METHODOLOGY

#### 3.1. Site Description

In this study, different study areas were selected to develop the prediction models. The first study area is a 14-km section of the main 420-km Desert Highway, which is the main highway running from the capital of Amman to the coastal city of Aqaba in the south part of Jordan. The road section starts from the Queen Alia International Airport interchange and extends to the Al-Dabaa zone in Al-Jiza County, with three lanes in each direction. The remaining study areas are located in the US states of Illinois, Indiana, and Minnesota, as well as AASHTO test road sections selected for studying flexible pavement performance. All data collected in the US also came from main arterials with three lanes per direction. Moreover, among the sections of selected pavements, all the various types and degrees of pavement distress were contained to influence the serviceability of highways.

The field measurements of the IRI data for the Desert Highway were collected using the Australian Road Research Board (ARRB) laser profiler. The measured IRI values were grouped into 50-m segments to achieve appropriate accuracy, represented by the average value of IRI in that segment. A total of 300 IRI values was evaluated along the selected highway section. The SV measurements were conducted using the CHLOE profilometer, which is a simplified profilometer developed by the road test staff. Thus, neither a chart reader nor a digital computer is required when the CHLOE profilometer is used. The purpose of this device is to obtain the profile slope at 6-in intervals. Two wheels with 9-in spaces are used to measure the SV as an angle in radiant. The SV values were measured for the same selected road sections along the Desert Highway. Therefore, 300 SV values were collected for this study

area. The maximum, minimum, and average IRI and SV values for the Desert Highway are shown in Tab. 1.

Table 1  
Maximum, Minimum, and Average IRI and SV Values for Jordan's Desert Highway

	Maximum	Minimum	Average
IRI (m/km)	9.20	1.00	3.16
SV	49.45	2.27	12.56

For the three US states, measurements were generated using the AASHTO road profiler, then an adaptation computer program provided by the World Bank was employed for the analysis process to calculate the IRI values. In total, 233 sets of IRI and SV data were used to develop the prediction model as follows: 10 data sets from Illinois, 95 from Minnesota, 74 from Indiana, and 54 from AASHTO road test sections. Each section was 1,200 ft (365.76 m) long, except those on the road test, which averaged 215 ft (65.5 m). The maximum, minimum, and average IRI and SV values for US states are shown in Tab. 2.

Table 2  
Maximum, Minimum, and Average IRI and SV Values for the US Highways

	Maximum	Minimum	Average
IRI (m/km)	7.39	0.76	2.52
SV	67.47	0.15	16.17

#### 4. ANALYSIS AND RESULTS

The IRI data were classified according to Sayers's [20] scale, along with the roughness level. Then, the surface conditions were determined. An IRI value below 2.0 was classified as an "excellent" condition, while a pavement with a high level of roughness was in "poor" condition when the IRI value was above 10. The frequency of each IRI scale is recorded and summarized in Fig. 1. The maximum IRI value of all the data points is 9.2 m/km, whereas the minimum IRI value was 1.00 m/km.

##### 4.1. GEP Model Development

In this study, two techniques were employed to develop a prediction model and establish an accurate and reasonable relationship between the IRI and SV. The first technique is an ANN-based technique, and the second is based on the GEP. The GEP is a specialized form of genetic programming that was developed to obtain a practical solution for prediction models. It involves a population of mathematical solutions that develop the best solution by an optimization process. It is considered an extension of the genetics algorithm technique. This technique was first developed by Koza [21] and was then improved as a main branch of GP by Ferreira [22]. Imam et al. [5] indicated that the GEP has a high potential to solve complex problems by employing a small population size. The GEP contains two languages to exhibit the solution: chromosomes and expression trees (ET), which represent the encoded information in the chromosome. The reading of the ET is straightforward (from left to right and from top to bottom). The head and intermediate nodes represent mathematical functions, while the tail nodes represent the independent variables or constant values.

The GeneXproTools 5 software package was used to build the GEP structure and find the best prediction model. In this study, the GEP model was composed of 30 chromosomes and two genes. The head and intermediate nodes represent mathematical functions, while the tail nodes represent the independent variables or constant values. In the model, the head and tail size were 7 and 8, respectively, and the linking function was addition. The selection of these parameters affects the generalization of the developed GEP model. A total of 50,000 generation processes was selected to optimize the parameters

that would be employed in the GEP model. The best tree-based model was simplified to a final formula including the desired input and output variables for predicting the output variable as presented in Fig. 2.

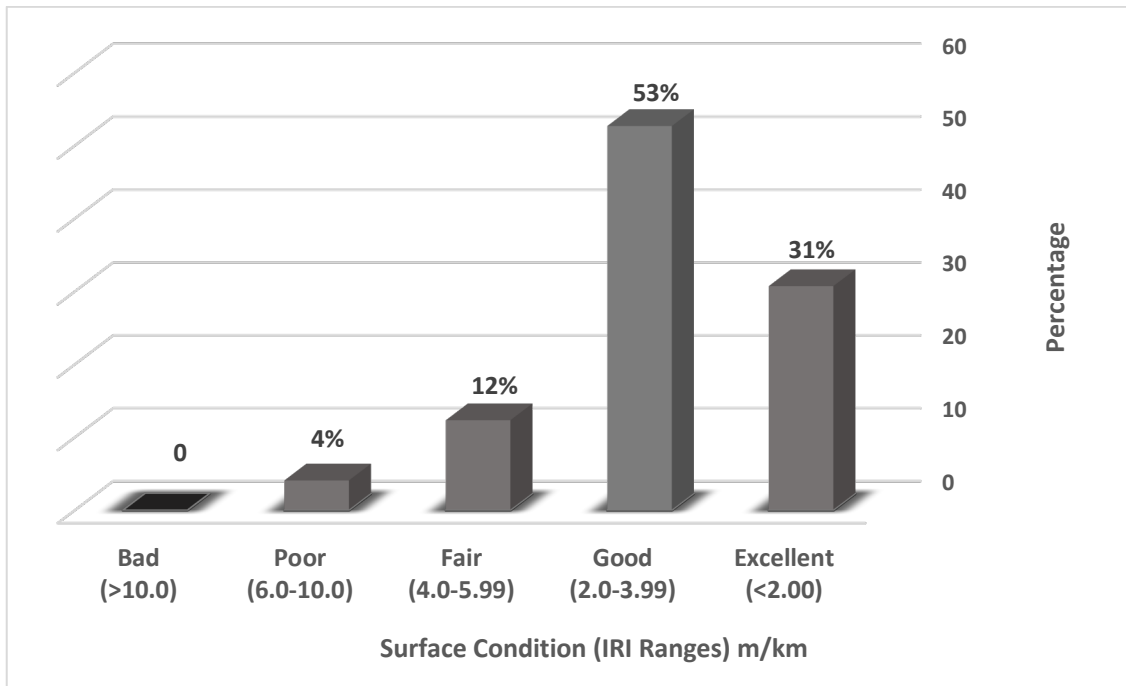


Fig. 1. Distribution of IRI Roughness Levels

In Fig. 2, the abbreviations used are as follows: Exp = expression, Inv = invert, Ln = natural logarithm, d0 = IRI, and c4, c7, c9 = the constants obtained from the GeneXproTools program results.

The final relationship using the GEP technique is presented in Eq. 6

$$SV = \left[ 2.83 - \left( \frac{1}{IRI} \right)^2 \right] + \left[ \left( \frac{1}{4.96 - IRI} + 4.9 + IRI \right) \times (Ln(IRI))^2 \right] \tag{6}$$

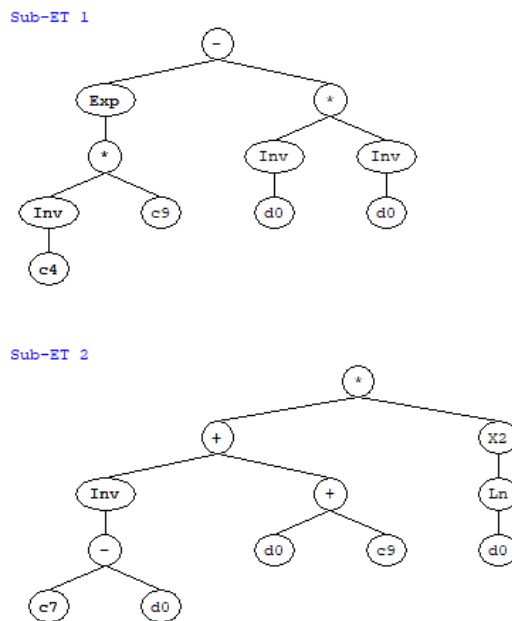


Fig. 2. Representation of the Expression Tree of the GEP Model

## 4.2. ANN Model Development

ANNs are well known as hardware or software intended and designed to execute specific tasks and assignments in various fields in the same way the human brain processes information using billions of operating units called neurons. The first initiation of the ANN was produced by McCulloch and Pitts in 1943. The ANN was described as a “massively parallel distribution process” since it can keep the information from data sets that are provided out of the network Bendana et al. [23]. ANNs require adaption and learning to perform effectively and accurately. In the mid-1980s, the ANN technique was introduced in many civil engineering fields and has since been widely and commonly used to solve complex problems and give precise and accurate solutions in computing fields [24]. The backpropagation and the Levenberg-Marquardt (LM) algorithms are the most popular techniques for training neural networks. ANN tools include three or more layers: an input layer that contains parameters, hidden layers that are used for delineating and learning the network pattern from the data, and the output layer. In this study, MATLAB 2019 (Math Work) was the software employed to develop the neural network approach. “MATLAB (an abbreviation of “matrix laboratory”) is a proprietary multi-paradigm programming language and numeric computing environment developed by MathWorks. MATLAB allows matrix manipulations, plotting of functions and data, implementation of algorithms, creation of user interfaces, and interfacing with programs written in other languages” [25].

The architecture of the developed neural network consists of an input layer, two hidden layers, and an output layer. The input and output layers each have one neuron, and the first and second hidden layers have 14 neurons each. The input layer contains one neuron representing the IRI values, while the output neuron represents the SV values. A schematic representation of the neural network is shown in Fig. 3.

The coefficient of determination ( $R^2$  value) was computed for all data sets, as well as the training and testing data records, to evaluate the performance of the developed GEP model. The  $R^2$  value of the complete data sets was equal to 0.9833 (Fig. 4). For the training data sets, the  $R^2$  was 0.9845 (Fig. 5), while the  $R^2$  value for the testing data was 0.9855 (Fig. 6).

As shown in the previous figures, the developed model gave more accurate results when the SV values were less than 35; when the SV value exceeds 35, the dispersion becomes larger from the trendline. The ANN-based model performance evaluation for complete data, training data, and testing data yielded high  $R^2$  values of 0.97, 0.968, and 0.98, respectively (Figs.7, 8, and 9). These values verify excellent prediction and a high correlation between the predicted and actual SV values.

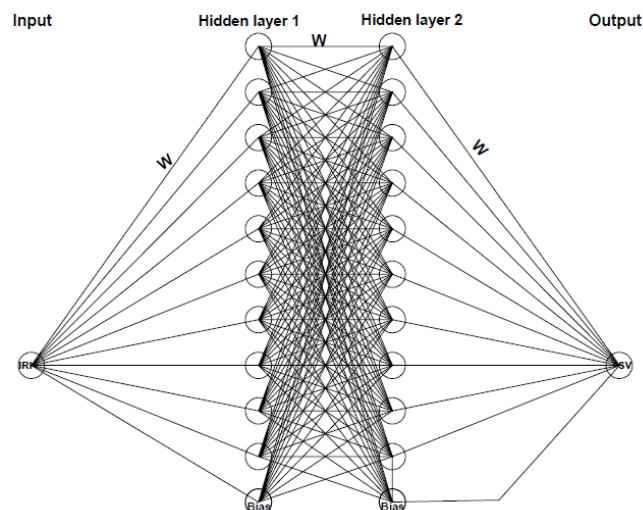


Fig. 3. Schematic Representation of a Neural Network

For quantifying the prediction error in terms of the units of the variable calculated by the model, Theil's inequality coefficient (U) was selected. Theil's inequality coefficient has become a standard validation tool adopted in various areas of scientific and engineering research [26]. The U-coefficient value was computed for both training and testing data according to Eq. 7.

$$U = \frac{\sqrt{\frac{1}{N} \sum_{n=1}^N (V_{o\ obs} - V_{o\ est})^2}}{\sqrt{\frac{1}{N} \sum_{n=1}^N (V_{o\ obs})^2} + \sqrt{\frac{1}{N} \sum_{n=1}^N (V_{o\ est})^2}} \tag{7}$$

where:  $V_{o\ obs}$  = Observed slope variance;  $V_{o\ est}$  = Estimated slope variance;  $N$  = the number of observations.

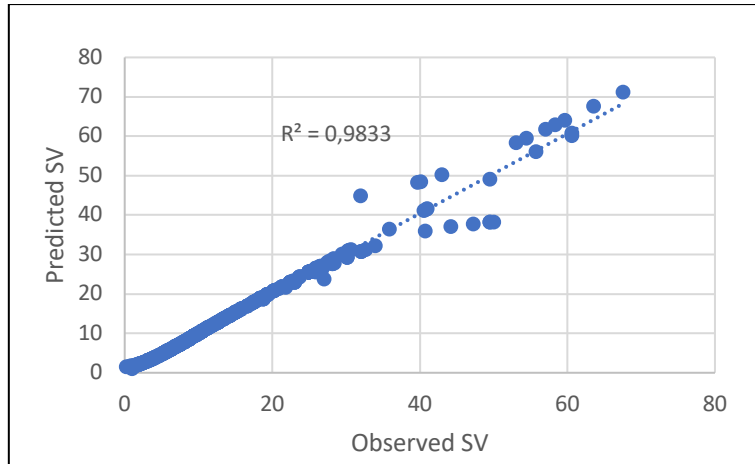


Fig. 4. Performance of the GEP Prediction Model for All Data Sets

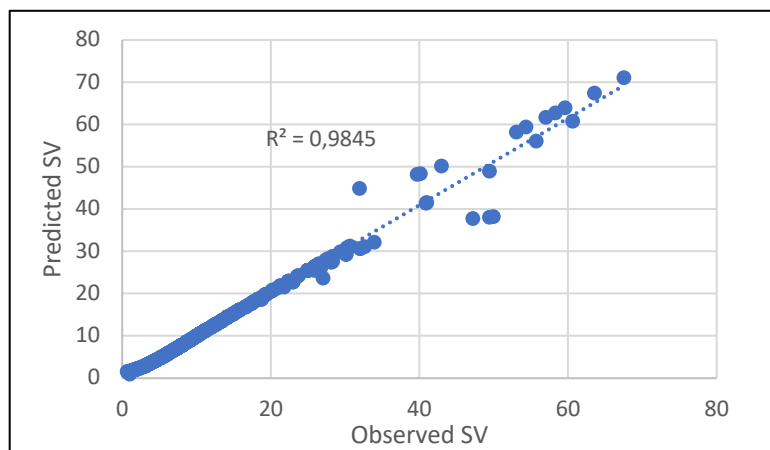


Fig. 5. Performance of the GEP Prediction Model for the Training Data

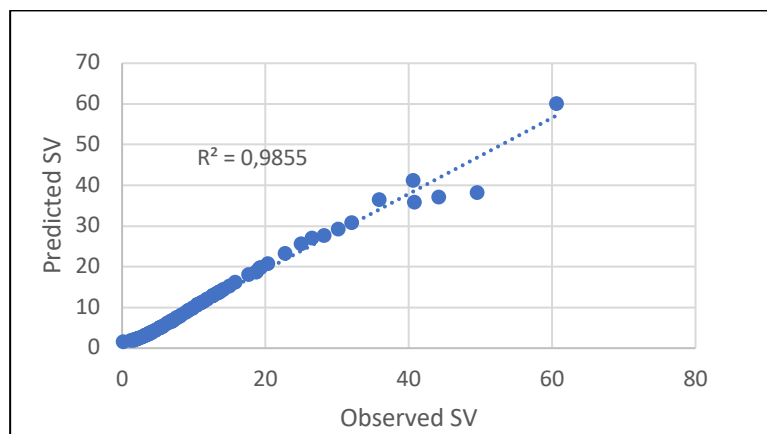


Fig. 6. Performance of the GEP Prediction Model for the Testing Data



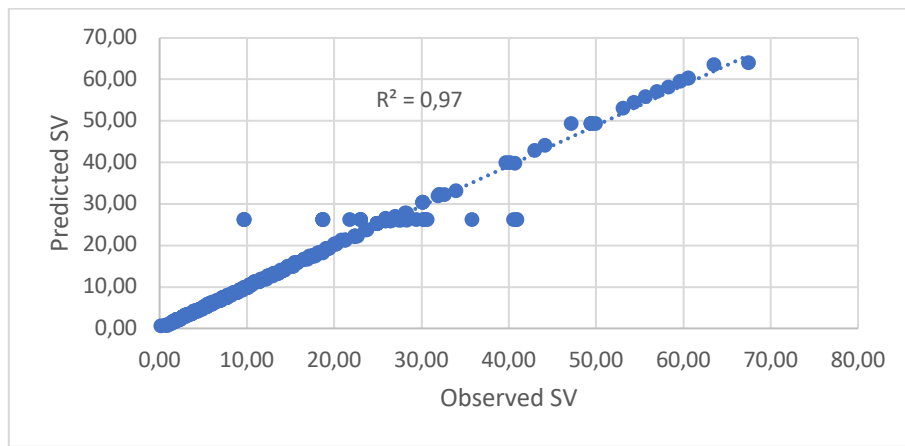


Fig. 7. Scatter Plot of Predicted vs. Observed SV for All Data with ANN Model

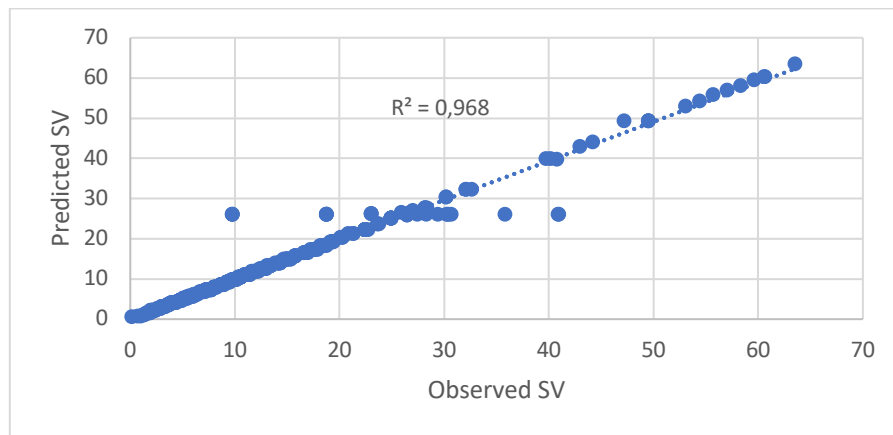


Fig. 8. Scatter Plot of Predicted vs. Observed SV Training Data with ANN Model

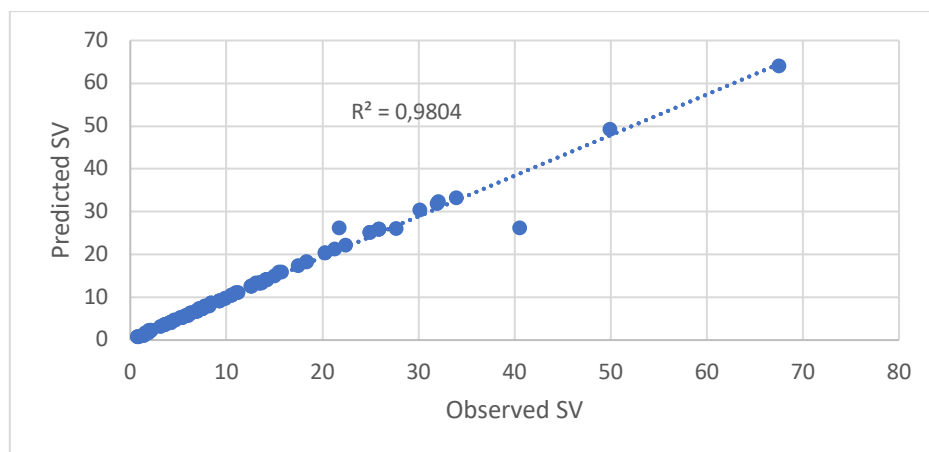


Fig. 9. Scatter Plot of Predicted vs. Observed SV of Testing Data with ANN Model

The U-values for the GEP and ANN models are presented in Tabs. 3 and 4, respectively. The U-values range from 0 to 1. A U-value of 0 indicates a perfect forecast, while a larger U-value reflects the model's poorer ability to predict accurately. A good predicting model should have a U-value of less than 0.3 [27]. U-values for both the training and testing data of both models were very small and close to zero, which indicates the high accuracy of the proposed models.

Table 3

## Summary of GEP Model Results

<b>GEP Model</b>			
<b>Data type</b>	<b>Training</b>	<b>Testing</b>	<b>All Data</b>
<b>Number of Data</b>	433	100	533
<b>Correlation Coefficient (R)</b>	0.992	0.993	0.992
<b>R<sup>2</sup></b>	0.9845	0.9855	0.9833
<b>Thiel's inequality coefficient (U) value</b>	0.04	0.05	0.04
<b>Average percentage error (%)</b>	3.8	2.6	3.8

Table 4

## Summary of ANN Model Results

<b>ANN Model</b>			
<b>Data type</b>	<b>Training</b>	<b>Testing</b>	<b>All Data</b>
<b>Number of Data</b>	433	100	533
<b>Correlation Coefficient (R)</b>	0.984	0.99	0.984
<b>R<sup>2</sup></b>	0.968	0.9804	0.97
<b>Thiel's inequality coefficient (U) value</b>	0.06	0.05	0.06
<b>Average percentage error (%)</b>	0.06	0.05	0.06

The paired t-test was employed to test whether the mean difference between pairs of measurements was zero for the training and testing data sets. The null and alternative hypotheses were as follows:

$H_0$  = The samples have the same means ( $\mu_1 = \mu_2$ )

$H_1$  = The samples have different means ( $\mu_1 \neq \mu_2$ )

$\mu_1$  is the population mean of variable 1, and  $\mu_2$  is the population mean of variable 2.

The final GEP and ANN model results for the complete, training, and testing data are summarized in Tabs. 5 and 6, respectively.

Table 5

## Summary of Paired t-test Results for Training and Testing for the GEP Model

<b>Paired Samples Test (GEP Model)</b>		
<b>Data</b>	<b>Training (Obs-Est)</b>	<b>Testing (Obs-Est)</b>
<b>Mean</b>	-0.0247	-0.0099
<b>Std. Deviation</b>	0.8151	1.5865
<b>Std. Error Mean</b>	0.0391	0.1586
<b>95% Confidence Interval of the Difference (Lower, Upper)</b>	(-0.1017,0.0523)	(-0.32473,0.3049)
<b>T</b>	-0.631	-0.062
<b>Df</b>	432	99
<b>Sig. (2-tailed)</b>	0.529	0.95

## 5. COMPARISON BETWEEN THE DEVELOPED PREDICTION MODELS

In this section, the GEP-based model, the ANN-based model, and previous models from published papers are compared to evaluate the performance of the developed models. The predicted SV values were computed using literature models. Two models were employed to produce the predicted SV values using all 533 data sets (Dujisin and Arroyo [17] and Hall and Muñoz [18]). Then, the results were compared with the actual SV.

Table 6

Summary of Paired t-test Results for Training and Testing for the ANN Model

<b>Paired Samples Test (ANN Model)</b>		
<b>Data</b>	<b>Training (Obs-Est)</b>	<b>Testing (Obs-Est)</b>
<b>Mean</b>	-0.05252	0.16938
<b>Std. Deviation</b>	1.98296	1.55737
<b>Std. Error Mean</b>	0.0953	0.15574
<b>95% Confidence Interval of the Difference (Lower, Upper)</b>	(-0.23982,0.13478)	(-0.13964,0.47839)
<b>T</b>	-0.551	1.088
<b>df</b>	432	99
<b>Sig. (2-tailed)</b>	0.582	0.279

The  $R^2$ , root mean square error (RMSE), mean absolute error (MAE), and U-coefficient value (using Eq. 7) were the statistical parameters used for comparing the GEP model, ANN model, and the previous models using the complete dataset based on Eqs. 8 and 9.

$$MAE = \frac{1}{N} \sum_{i=1}^N |P_i - O_i| \quad (8)$$

$$RMSE = \sqrt{\frac{\sum_{i=1}^N (P_i - O_i)^2}{N}} \quad (9)$$

where: P and O =the predicted and observed values.

Fig. 10 presents the comparison between the observed SV values and the predicted SV values computed by the GEP model, ANN model, and two previous literature models for the complete 533 data records. The GEP model recorded the highest  $R^2$  value (98.3%) among all models, followed by the ANN-based model ( $R^2 = 97\%$ ). Meanwhile, the previous statistical models achieved the lowest  $R^2$  values of 88.3% and 81.7%. This indicates that the developed GEP and ANN models in this study outperformed the previous models. Thus, the developed models in this study are the first GEP and ANN models to establish the IRI-SV relationship efficiently and accurately, allowing the next essential step in predicting the PSI for road sections. The summarized results of the statistical performance parameters for all the prediction models are presented in Tab. 7.

The results in Tab. 7 show that the previous models recorded higher error percentages than the two models proposed in this research. Regarding the model of Hall and Muñoz [18], the U-coefficient value was the highest because the slope variance in their model was calculated by squaring the IRI value (as shown in Eq. 5). Thus, when the IRI values are high, the difference between the actual and estimated slope variance becomes high, and, in turn, the U-coefficient depends on the difference between these two values.

## 6. CONCLUSIONS AND RECOMMENDATIONS

The main objective of this study was to develop a relationship between IRI and the SV for flexible pavements using ANN and GEP techniques. A comprehensive statistical analysis was conducted to validate the developed models, evaluate their performance, and determine their suitability. According to the IRI values, the condition of the pavement surface is “excellent” when the value of SV is less than 6, while the surface condition of the pavement tends to be “very poor” or “critical” when SV exceeds 70 since this means the level of road roughness is high. The results of the obtained GEP model were evaluated by calculating  $R^2$  for all data, training data, and testing data, which were equal to 0.983, 0.985, and 0.986, respectively. Furthermore, the ANN model performed well, with excellent  $R^2$  values. The  $R^2$  values for the complete data set, training data set, and testing data set were 0.97, 0.968, and 0.98, respectively. U-values were computed for both the ANN-based model and the GEP-based model for the training and testing data. For the GEP model, the U-values for the training and testing were 0.04 and 0.05, respectively; for all data, this value was 0.04. Similarly, the U-values for the ANN model were

0.05, 0.06, and 0.05 for the training, testing, and complete data sets, respectively. These values are close to zero, indicating high accuracy and perfect fitness. Moreover, the paired t-test was performed to determine the precision of the developed models. All significance values were greater than 0.05; thus, the null hypothesis was not rejected, which indicates that the predicted SV values were not significantly different from the actual SV values. In terms of forecasting the SV values from IRI input values, both the GEP and ANN models reliably and accurately related these parameters, which confirms their ability to predict SV. SV is an essential roughness parameter required in PSI calculations for road sections.

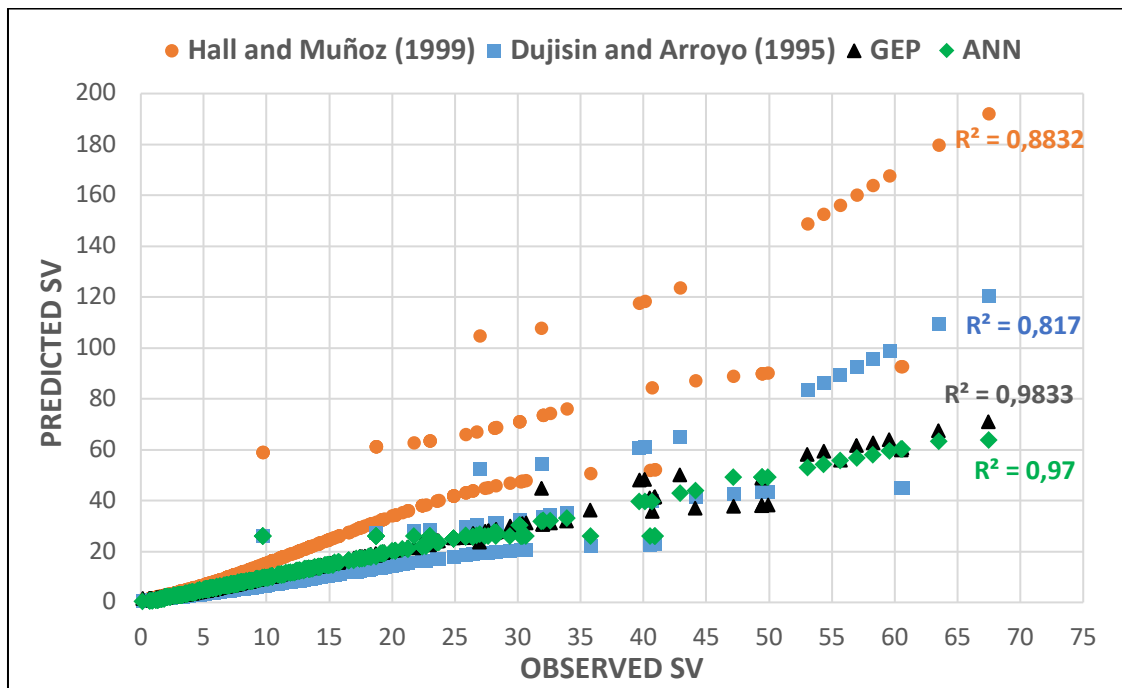


Fig. 10. Comparison between the Observed and Predicted SV Using Different Models

Table 7

Summary of Statistical Performance Parameters

Prediction Model	U-coefficient value	R <sup>2</sup>	RMSE (%)	MAE (%)
Dujisin and Arroyo (1995)	0.192	0.82	6.64	3.84
Hall and Muñoz (1999)	0.382	0.88	19.82	10.40
GEP-Based model	0.04	0.98	1.46	0.50
ANN-Based model	0.06	0.97	1.91	0.44

Based on the findings of this study, the developed ANN and GEP models showed high correlations between the IRI and the SV. The IRI field measurement process and devices are less expensive and easier than the SV measurement process. Moreover, IRI data is more accessible for various pavement road sections due to the availability of IRI measuring devices. Therefore, the need to use the IRI data to predict the SV values is apparent as an important indicator of road roughness. SV can be used to estimate the PSI, which is one of the most common pavement performance measures used for evaluating current and future conditions and maintenance requirements of large-scale highway networks. Prediction models of road roughness indices are valuable since such relationships enable pavement engineers to transfer one index to another without the need for additional field measurements. Therefore, such models could save highway agencies significant money and time. A parametric study on the proposed models could be performed using different data sets to further validate the developed models. Additionally, it is recommended to investigate the validity of the developed models for pavements of variable ages, as well as different weather and traffic conditions.

## References

1. Msallam, M. & Al Rawi, O.S. & Abudayyeh, D. & Assi, I. Development of a pavement management system to be used in highway pavement evaluation in Jordan. *Development*. 2014. Vol. 6. No. 9. P. 330-342.
2. Highway Research Board, *The AASHO Road Test, Report 5, Pavement Research*. Special Report 61E, Publication No. 954. National Academy of Sciences – National Research Council, Washington, D.C. 1962.
3. Wei, L. & Fwa, T.F. Characterizing road roughness by wavelet transform. *Transportation Research Record*. 2004. Vol. 1896. No. 1. P. 152-158.
4. Chang, J.R. & Su, Y.S. & Huang, T.C. & Kang, S.C. & Hsieh, S.H. Measurement of the international roughness index (IRI) using an autonomous robot (P3-AT). In: *26<sup>th</sup> International Symposium on Automation and Robotics in Construction*. 2009. Vol. 130. No. 1. P. 325-331.
5. Imam, R. & Murad, Y. & Asi, I. & Shatnawi, A. Predicting Pavement Condition Index from International Roughness Index using Gene Expression Programming. *Innovative Infrastructure Solutions*. 2021. Vol. 6. No. 3. DOI: 10.1007/s41062-021-00504-1.
6. Carey Jr, W.N. & Huckins, H.C. & Leathers, R.C. Slope Variance as a Measure of Roughness and the CHLOE Profilometer. *HRB Spec*. 1962. Vol. 73. No. 1. P. 126-137.
7. Yunusov, A. & Riskaliev, D. & Abdugarimov, N. & Eshkabilov, S. Signal processing and conditioning tools and methods for road profile assessment. In: *Design, Simulation, Manufacturing: The Innovation Exchange*. 2019. P. 742-751.
8. Islam, S. & Buttlar, W.G. & Aldunate, R.G. & Vavrik, W.R. Measurement of pavement roughness using android-based smartphone application. *Transportation Research Record*. 2014. Vol. 2457. No. 1. P. 30-38.
9. Arhin, S.A. & Williams, L.N. & Ribbiso, A. & Anderson, M.F. Predicting pavement condition index using international roughness index in a dense urban area. *Journal of Civil Engineering Research*. 2015. Vol. 5. No. 1. P. 10-17.
10. Azim, I. & Yang, J. & Javed, M.F. & Iqbal, M.F. & Mahmood, Z. & Wang, F. & Liu, Q.F. Prediction model for compressive arch action capacity of RC frame structures under column removal scenario using gene expression programming. *Structures*. 2020. Vol. 25. No. 1. P. 212-228.
11. Murad, Y. & Imam, R. & Hajar, H.A. & Hammad, A. & Shawash, Z. (2019). Predictive compressive strength models for green concrete. *International Journal of Structural Integrity*. 2019. Vol. 11. No. 2. P. 169-184. DOI: 10.1108/IJSI-05-2019-0044.
12. Choi, J. & Adams, T.M. & Bahia, H.U. Pavement Roughness Modelling Using Back-Propagation Neural Networks. *Computer-Aided Civil and Infrastructure Engineering*. 2004. Vol. 19. No. 4. P. 295-303.
13. Vidya, R. & Santhakumar, S.M. & Mathew, S. Estimation of IRI from PCI in construction work zones. *International Journal on Civil and Environmental Engineering*. 2013. Vol. 2. No. 1. P. 1-5.
14. Hossain, M.I. & Gopiseti, L.S.P. & Miah, M.S. International Roughness Index Prediction of Flexible Pavements Using Neural Networks. *Journal of Transportation Engineering, Part B: Pavements*. 2019. Vol. 145. No. 1. P. 1-10.
15. Mazari, M. & Rodriguez, D.D. Prediction of Pavement Roughness using a Hybrid Gene Expression Programming-Neural Network Technique. *Journal of Traffic and Transportation Engineering*. 2016. Vol. 3. No. 5. P. 448-455.
16. Bayrak, M.B. & Teomete, E. & Agarwal, M. Use of Artificial Neural Networks for Predicting Rigid Pavement Roughness. In: *Midwest Transportation Consortium Fall Student Conference*. Ames, Iowa, USA. 2004.
17. Dujisin, D. & Arroyo, A. Developing a relationship between present serviceability index – International Roughness Index. *Chilean Chamber of Construction*. Santiago, Chile. 1995.
18. Hall, K. & Muñoz, C. Estimation of present serviceability index from international roughness index. *Transportation Research Record*. 1999. Vol. 1655. No. 1. P. 93-99.

19. Shahnazari, H. & Tutunchian, M.A. & Mashayekhi, M. & Amini, A.A. Application of Soft Computing for Prediction of Pavement Condition Index. *Journal of Transportation Engineering*. 2012. Vol. 138. No. 12. P.1495-1506.
20. Sayers, M. & Gillespie, T.D. & Paterson, W.D.O. *Guidelines for the Conduct and Calibration of Road Roughness Measurements*. Technical Report No. 46. Washington, D.C. 1986.
21. Koza, J.R. Genetic programming as a means for programming computers by natural selection. *Statistics and computing*. 1994. Vol. 4. No. 2. P. 87-112.
22. Abambres, M. & Ferreira, A. *Application of ANN in Pavement Engineering: State-of-Art*. 2017.
23. Bendana, R. & Del Cano, A. & De la Cruz, M.P. Contractor selection: Fuzzy-control approach. *Canadian Journal of Civil Engineering*. 2008. Vol. 35. No. 5. P. 473-486.
24. Flood, I. & Kartam, N. Neural networks in civil engineering: Principles and understanding. *Journal of Computing in Civil Engineering*. 1994. Vol. 8. No. 2. P. 131-148.
25. Eaton, J. W. Octave: Past, present and future. In: *Proceedings of the 2<sup>nd</sup> International Workshop on Distributed Statistical Computing*. 2001. Vienna, Austria.
26. Rowland, J.R. & Holmes, W.M. Simulation validation with sparse random data. *Computers & Electrical Engineering*. 1978. Vol. 5. No. 1. P. 37-49.
27. Toledo, T. & Koutsopoulos, H.N. Statistical validation of traffic simulation models. *Transportation Research Record*. 2004. Vol. 1876. No. 1. P.142-150.

Received 22.01.2021; accepted in revised form 20.05.2022